Shaft resistance capacity of axially loaded piles in cohesive-frictional soils under static or pseudo-static conditions based on ground parameters

Lysandros Pantelidis (lysandros.pantelidis@cut.ac.cy)
Cyprus University of Technology https://orcid.org/0000-0001-5979-6937

Research Article

Keywords: shaft resistance of piles, effective stress analysis, pile-soil interaction, earth pressure at-rest, cohesive-frictional soils, pseudo-static analysis

Posted Date: August 24th, 2022

DOI: https://doi.org/10.21203/rs.3.rs-1986330/v1

Shaft resistance capacity of axially loaded piles in cohesive-frictional soils under static or pseudo-static conditions based on ground parameters

Lysandros Pantelidis[1,*]

[1] Cyprus University of Technology, 3036 Limassol, CY

* lysandros.pantelidis@cut.ac.cy

Abstract

According to the current practice, the unit shaft resistance of piles based on ground parameters is calculated with the α-method or the β-method, for total or effective stress conditions respectively. Indeed, these two methods are included in the prEN1997-3:2021 draft standard. And while the physics behind these methods is adequate for calculating the shaft resistance of piles in clays and sands for total and effective stress analysis respectively, the main difficulty in applying the effective stress approach in clays is to estimate the radial effective stress acting on the pile. In the present paper this is addressed by a proposed earth pressure at-rest coefficient, applicable to cohesive-frictional soils and both horizontal and vertical pseudo-static conditions. Comparison examples show excellent agreement of the analytically derived shaft resistance capacities with the respective numerical ones. Regarding seismic conditions it is noted that, for the case of axially loaded piles the horizontal component of the seismic excitation does not affect the shaft resistance capacity of piles, while the vertical component could be neglected as acting favorably. Finally, it is mentioned that the proposed method is a general $c - \varphi$ procedure, applicable also for purely cohesive and cohesionless soils.

Keywords: shaft resistance of piles, effective stress analysis, pile-soil interaction, earth pressure at-rest, cohesive-frictional soils, pseudo-static analysis

1 Introduction

In 2019, the author (Pantelidis, 2019) proposed a continuum mechanics approach for deriving earth pressure coefficients for any soil state between the “at-rest” state and the active state,

applicable to cohesive-frictional soils and both horizontal and vertical pseudo-static conditions. The basic earth pressure coefficient expression is:

$$K_{XE} = \frac{1-\sin\varphi'}{1+\sin\varphi'}\left((1-\xi\cdot\sin\varphi') + \frac{k_h}{1-k_v}\cdot\tan\varphi'\left(2+\xi\cdot(1-\sin\varphi')\right)\right) - \frac{1}{1-k_v}\frac{2c_m}{\gamma z}tan\left(45^o-\frac{\varphi'}{2}\right) \quad (1)$$

with $\xi = (\mathrm{m}-1)/(\mathrm{m}+1)-1$, while the soil state is controlled by the parameter m (m is real positive number ranging between 1 and ∞). As m tends to infinity, K_{XE} approaches the active earth pressure coefficient for seismic situation:

$$K_{AE} = \frac{1-\sin\varphi'}{1+\sin\varphi'}\left(1+2\frac{k_h}{1-k_v}\cdot\tan\varphi'\right) - \frac{1}{1-k_v}\frac{2c_m}{\gamma z}\tan\left(45^o-\frac{\varphi'}{2}\right) \quad (2)$$

Under static conditions ($k_h = k_v = 0$), the (analytically) calculated mobilized cohesion, c_m, is equal to its peak value, c' (Pantelidis, 2019) and thus, Equation 2 leads to the well-known Rankine's (1857) expression for active earth pressures (with Bell's, 1915, extension for cohesion).

By just setting $m = 1$, Equation 1 gives the generalized coefficient of earth pressure at-rest:

$$K_{OE} = (1-\sin\varphi')\left(1+\frac{k_h}{1-k_v}\cdot\tan\varphi'\right) - \frac{1}{1-k_v}\frac{2c_m}{\gamma z}\tan\left(45^o-\frac{\varphi'}{2}\right) \quad (3)$$

In Rankine's form, the latter can be rewritten as follows:

$$K_{OE} = \frac{1-\sin\varphi_m}{1+\sin\varphi_m} - \frac{2c_m}{\gamma_m z}\tan\left(45^o-\frac{\varphi_m}{2}\right) \quad (4)$$

with $\tan\varphi_m = SMF\cdot\tan\varphi'$, $c_m = SMF\cdot c'$ and $\gamma_m = (1-k_v)\gamma$. It is apparent that, under Jaky's assumptions (static situation and cohesionless soils), Equation 3 leads to Jaky's (1948)

well-known $Ko = 1 - \sin\varphi'$ expression. Jaky's (1944) $Ko = (1 - \sin\varphi')(1 + ⅔\sin\varphi')/(1 + \sin\varphi')$ derives also from Equation 1 for $m = 2$ (also $k_h = 0$ and $c' = 0$), corresponding to an intermediate state between the at-rest state and the active state.

For cohesive-frictional soils, the mobilized shear strength parameters of soil (c_m, φ_m) are calculated using the analytical procedure or the charts given in Pantelidis (2019). For the special case of purely frictional soils, the at-rest mobilized friction angle can be calculated as follows:

$$\varphi_m = ArcSin\left[\frac{1-(1-\sin\varphi\prime)(1+\tan\theta_1\tan\varphi\prime)}{1+(1-\sin\varphi\prime)^2(1+\tan\theta_1\tan\varphi\prime)}\right] \quad (5)$$

Knowing the coefficient of earth pressure at-rest at depth z, the respective earth pressure is:

$$\sigma_{OE} = K_{OE}(1 - k_v)\gamma z \quad (6)$$

Also, it is reminded that, a neutral zone (zone where soil exerts no pressure on the structure, e.g., retaining wall, pile) is extended from soil's surface to depth z_{nz} (Equation 7) because soil's cohesion (if any).

$$z_{nz} = \frac{c'}{(1-k_v)\gamma\tan\varphi'}\left[\frac{1}{\left(\cos\varphi' + \frac{k_h}{1-k_v}\sin\varphi'\right)^2} - 1\right] \quad (7)$$

An exhaustive validation of Pantelidis' (2019) continuum mechanics approach against contemporary centrifuge tests and finite elements can be found in Pantelidis and Christodoulou (2022); the same paper also presents an in-depth evaluation of the earth pressure methods included in EN1998-5:2004 (use of Mononobe-Okabe method; Mononobe and Matsuo, 1929; Okabe, 1926), prEN1998-5:2021 and AASHTO (use of the M-O method with half peak ground acceleration; AASHTO American Association of State Highway and Transportation Officials, 2010).

The above formulae will be used herein for introducing a new method for calculating the shaft resistance capacity of piles in cohesive-frictional soils, under pseudo-static conditions, based on ground parameters. The current practice is the use of the following equations for total and effective stress conditions respectively:

$$q_s = \alpha c_u \tag{8}$$

$$q_s = \beta \sigma'_v \tag{9}$$

Equations 8 and 9 are best-known as the α-method and the β-method respectively. α is an adhesion factor for piles in soil, $\beta = K_s \tan\delta$ is an empirical coefficient, K_s is an earth pressure coefficient, while δ is the friction angle of the pile – ground interface. K_s is usually Jaky's (1948) $K_O = 1 - \sin\varphi'$, unless the soil is over-consolidated or a pile driven in the soil causes the over-consolidation of the latter in the very close vicinity around it. For over-consolidated soils an empirical value K_s is used (e.g., Mayne and Kulhawy, 1982). Equations 8 and 9 have been proposed by Tomlinson (1957) and Burland (1973). It is also mentioned that, Equations 8 and 9 reflect the current best-practice for "fine soils and fills" (see draft standard prEN1997-3:2021, 2021).

And while the physics behind Equations 8 and 9 is adequate for calculating the shaft resistance of piles in clays (for total stress analysis) and sands (for effective stress analysis) respectively, the main difficulty in applying the effective stress approach (i.e. Equation 9) in clays is to estimate the radial effective stress on the pile, that is, the coefficient K_s (Tien, 1981). The purpose of the present paper is to suggest a new, reliable method for calculating the shaft resistance in cohesive-frictional soils (effective stress analysis in clays) focusing on the stress field around the pile; the empirical derivation of any adhesion factor a or friction angle δ for the pile-soil

89 interface is out of the scopes of the present paper; besides, numerous researchers have already
90 made their contribution in this area (such values can be found e.g., in API, 2000; Tien, 1981).

91 2 Proposed analytical procedure for the calculation of the shaft resistance of axial
92 loaded piles

93 There is no doubt that the vertical component of a seismic excitation increases (or decreases,
94 depending on the direction of ground acceleration) the weight of the pile, as well as of the
95 superstructure. The same also stands for the soil around a pile, where during the cyclic action
96 of an earthquake, the soil becomes heavier, lighter, and so on. Adopting the commonly used
97 pseudo-static approach, the unit weight of soil will be $(1 \mp k_v)\gamma$ (minus for a downward seis-
98 mic acceleration and vice versa). In turn, the unit weight of soil (as adapted to the vertical
99 seismic situation) affects the earth pressures at-rest (recall Equation 6).
100 Regarding the horizontal component of seismic excitation, a pile inside the ground interrupts
101 the continuity of the latter along the horizontal direction and since its unit weight is greater
102 than the unit weight of the surrounding soil, it acts as inertial mass with different period of
103 vibration, T. Since T is proportional to mass (i.e., to unit weight), and the unit weight of a
104 concrete or steel pile is greater than the unit weight of soil, the pile will be keep moving for a
105 bit longer, while the soil is already returning towards its first full oscillation (and so on). Alt-
106 hough this lag may potentially trigger a passive failure condition, the oscillating nature of the
107 problem and the rather non-significant difference in the unit weights (at least when dealing
108 with reinforced concrete or steel pipe piles), will not allow for this to occur; besides, a passive
109 failure requires a significant amount of displacement. Given the above and based on the com-
110 mon engineering experience, the rational assumption that the pile retains its initial position can
111 be made and thus, all earth pressures acting on it are earth pressures “at-rest”, which act radially

on a circular pile. However, the direction of the horizontal seismic excitation defines the direction for the analysis. In this respect, only the pseudo-static earth pressure components parallel to the direction of the horizontal seismic excitation contribute to a possible horizontal pile movement; thus, the pile is divided into an "active" and a "passive side", affected by a positive and negative pseudo-static coefficient respectively (Figure 1). These earth pressure components will have value $K_{OE}\gamma z\cos\theta$; the symbol K_{OE}^{+} hereinafter means earth pressure coefficient at-rest for a positive k_h value, while the K_{OE}^{-} for a negative pseudo-static horizontal coefficient (i.e., $-k_h$). Therefore, and referring to the "active side" of the problem, the resultant earth pressure "at-rest" force acting on the curved surface area of a circular pile will be:

$$P_{OE}^{+} = \int_{z=0}^{z=H}\int_{-\pi/2}^{\pi/2}[K_{OE}^{+}(1-k_v)\,\gamma\,z\,R\,\cos\theta]d\theta\,dz = (2R)\frac{K_{OE}^{+}\,\gamma\,(1-k_v)H^2}{2} \quad (10)$$

That is, the problem is reduced to earth pressures acting on a vertical, planar diaphragm with surface area $2R\cdot H$. Equation 10 refers to the half, curved surface area of the pile, as indicated by the limits of the integral from $-\pi/2$ to $\pi/2$ and to a positive k_h value (K_{OE}^{+}). A resultant earth pressure force P_{OE}^{-} equal to $K_{OE}^{-}\,\gamma\,(1-k_v)H^2$ acts on the opposite ("passive") side (use of K_{OE}^{-} with $-k_h$).

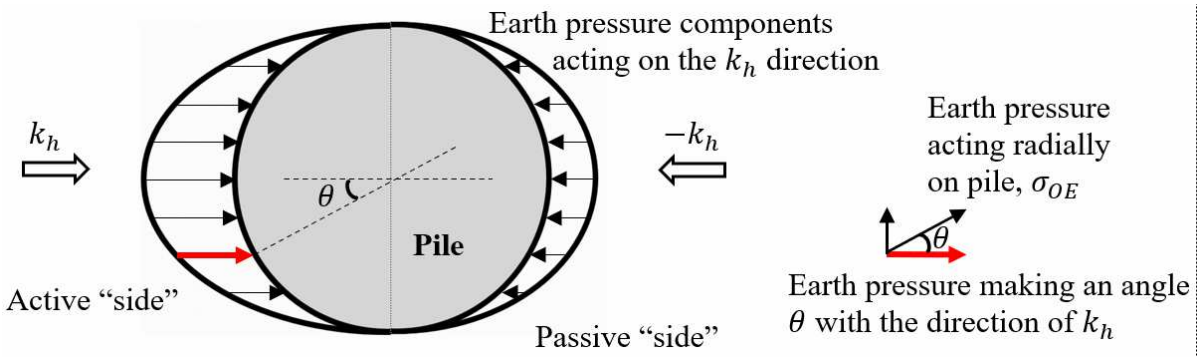

Figure 1. Earth pressure at-rest components acting on the k_h direction (horizontal cross section).

From the above it is inferred that the total normal force acting on both sides of the pile is

$$P_{OE} = P_{OE}^{+} + P_{OE}^{-} = (2R)\frac{K_{OE}^{+}+K_{OE}^{-}}{2}\gamma(1-k_v)H^2 \qquad (11)$$

And with the use of Equation 3, the latter simplifies to

$$P_{OE} = (2R)\left(1-\sin\varphi' - \frac{1}{1-k_v}\frac{2c_m}{\gamma z}\tan\left(45^o - \frac{\varphi'}{2}\right)\right)\gamma(1-k_v)H^2 \qquad (12)$$

That is, the earth pressures that will act radially around the pile, on average, will correspond to an "at-rest" coefficient

$$K_{OE} = 1 - sin\varphi' - \frac{1}{1-k_v}\frac{2c_m}{\gamma z}tan\left(45^o - \frac{\varphi'}{2}\right) \qquad (13)$$

Equation 13 is valid only for the case of axially loaded piles. Also, due to its favorable contribution, the vertical component of the seismic excitation could be neglected; a k_v pseudo-static coefficient acting downwards, increases the weight of the pile and of the superstructure (unfavorable action), while increasing the shearing resistance (favorable action; such actions can be neglected for the sake of safety).

Example curves for K_{OE}^{+}, K_{OE}^{-} and their average against depth are shown in Figure 2 for a cohesive-frictional soil (data: c'=40 kPa, φ'=10°, γ=20 kN/m^3, k_v=0 and k_h=±0.3). For convenience in applying the proposed method in cohesive-frictional soils, SMF and K_{OE} values are given in tabular form in the appendix.

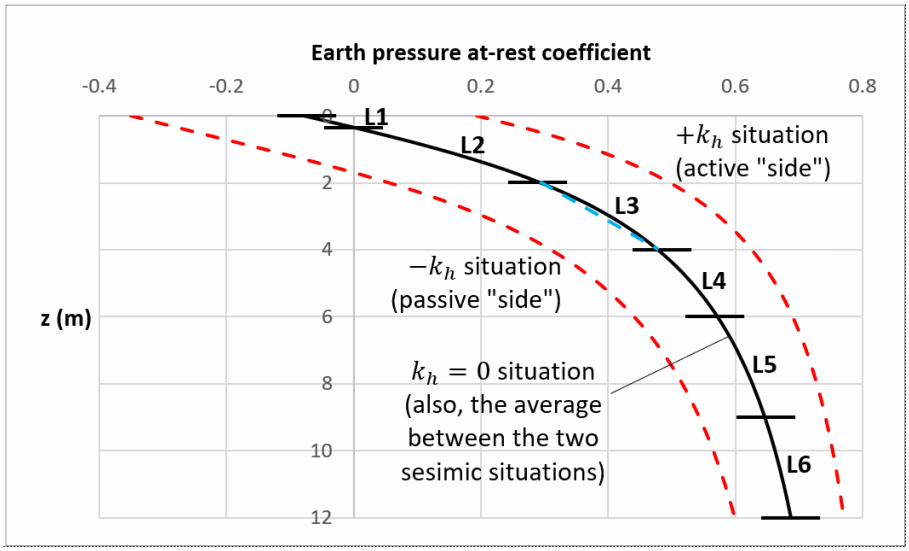

Figure 2. Earth pressure at-rest coefficient, K_{OE}, against depth, z, chart. The three K_{OE}-z curves have been drawn for k_h=-0.3, k_h=0and k_h=+0.3 (left to right; + for the active side and – for the passive side). Also, c'=40 kPa, φ'=10° and γ=20 kN/m3.

An application example of the proposed method follows. Let a 12-meter-long pile of one meter diameter in a homogenous soil medium with c'=40 kPa, φ'=10° and γ=20 kN/m^3. The pile is infinitively stiff, while the interface shear strength is defined by Equations 14 and 15 with shear reduction coefficient α_i being equal to 1, 2/3 or 1/3. Static conditions are considered (k_h=k_v=0).

$$c_{int} = \alpha_i \cdot c' \tag{14}$$

$$tan\varphi_{int} = \alpha_i \cdot tan\varphi' \tag{15}$$

The K_{OE} coefficient, as this varies with depth is shown in Figure 2 with black continues curve. K_{OE} remains negative up to depth equal to 0.353 m where soil exerts no lateral pressure (recall Equation 7; depth of neutral zone due to cohesion). Negative values in the analysis, apparently, are replaced with zero, assuming that soil receives no tension. Commenting on Figure 2, K_{OE} increases non-linearly with depth, reaching a value equal to 0.498 at the lowest point of the pile, before tending to an asymptotic value equal to 0.826 at infinite depth. For facilitating hand-calculations, the soil mass is divided into six layers, just for representing the $K_{OE} - z$

relationship with an equal number of straight lines (such a straight line has been drawn for layer 3; indicated as L3 in Figure 2). The higher and the lower z-coordinate of each layer are given in columns 1 and 4 of Table 1 respectively, while the respective *SRF* and K_{OE} values in columns 2, 3, 5 and 6. The average K_{OE} value for each layer is given in column 7, while columns 8 and 9 give the thickness and the average depth of each layer. The shaft resistance capacity force $Q_{s,i}$ corresponding to each sublayer is calculated using Equation 16, while the derived values are shown in column 10 of Table 1.

$$Q_{s,i} = \pi \cdot 2R \cdot \Delta z_i \cdot \alpha_i \left(c' + \overline{K_{OE}}_i \cdot \gamma \cdot \bar{z}_i \cdot tan\varphi'\right) \quad (16)$$

The maximum unfactored axial loading corresponding to the total shaft resistance of pile derives from Equation 17, and for the given example, it is equal to 2518.5 kPa, 1679.0 kPa and 838.7 kPa for $\alpha_i = 1$, 2/3 and 1/3 respectively.

$$q_{s,tot} = \sum_{i=1}^{6} \left[Q_{s,i} / \pi R^2\right] \quad (17)$$

Table 1. Table for the calculation of the total resistance of pile shaft based on the proposed method. Asymptotic values (i.e., for z→∞): SMF=0.542, K_{OE}=0.826.

z_{up} (m)	*SMF*	$K_{OE,up}$*	z_{down} (m)	*SMF*	$K_{OE,down}$	$\overline{K_{OE}}$	Δz (m)	$\bar{z}$ (m)	$Q_{s,i}$ (kN)		
									α_i=1	α_i =2/3	α_i =1/3
col.1	col.2	col.3	col.4	col.5	col.6	col.7	col.8	col.9	col.10	col.11	col.12
0	0	(-0.079)	0.353	0.087	0	0	0.343	0.18	43.1	28.7	14.4
0.353	0.087	0	2	0.318	0.293	0.1465	1.647	1.18	210.1	140.1	70.0
2	0.318	0.293	4	0.415	0.478	0.3855	2	3	277.0	184.6	92.2
4	0.415	0.478	6	0.455	0.572	0.525	2	5	309.5	206.3	103.1
6	0.455	0.572	9	0.484	0.646	0.609	3	7.5	528.8	352.5	176.1
9	0.484	0.646	12	0.498	0.687	0.6665	3	10.5	609.6	406.4	203.0
				Total shaft resistance force, Q_s (kN)					1978.1	1318.7	658.7
				Total resistance of pile shaft, $q_{s,tot}$ (kPa)					2518.5	1679.0	838.7

* Negative K_{OE} values in the calculations of the shaft resistance of pile are replaced with zero.

3 Numerical against analytical results

3.1 Shaft resistance capacity of pile in a c'=40 kPa, φ'=10° soil

The analytical example presented above is used herein for the necessary numerical validation of the proposed method. The numerical results were obtained using Rocscience's RS2; RS2 is a commercial program for 2D finite element analysis of geotechnical structures for civil and mining applications. The geometry and boundary conditions, as well as the mesh and the basic settings used are all shown in Figure 3. More specific data for the pile, soil and pile-soil interface can be found in Table 2.

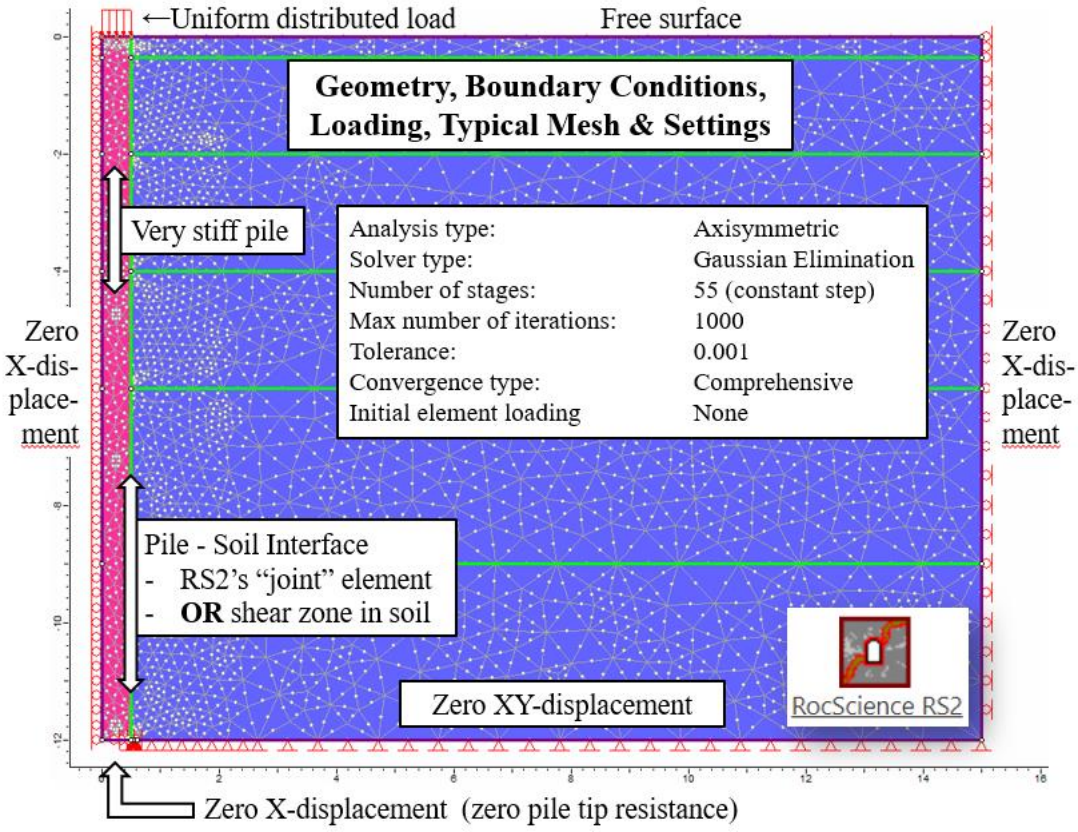

Figure 3. Geometry, boundary conditions, mesh and basic settings for the example used.

Table 2. Pile, pile-soil interface and soil data for Examples 1-6.

Element →	Pile	Pile-soil interface						Soil
		Shear zone	RS2's "joint" interface element					
Parameter ↓ Example →	All	#1	#2	#3	#4	#5	#6	All
Material type	Elastic / Isotropic	Plastic / Isotropic	-	-	-	-	-	Plastic / Isotropic
Unit weight (kN/m³)	0.0001	20	-	-	-	-	-	20
Poisson's ratio	0.2	0.3	-	-	-	-	-	0.3
Young Modulus (GPa)	10	0.02	-	-	-	-	-	0.02
Peak cohesion (kPa)	-	40	40	40	40	26.7	13.32	40
Peak friction angle (°)	-	10	10	10	10	6.7	3.36	10
Residual cohesion (kPa)	-	40	40	40	40	26.7	13.32	40
Residual friction angle (°)	-	10	10	10	10	6.7	3.36	10
Shear reduction coef., α_i	-	1	1	1	1	2/3	1/3	-
Normal Stiffness (GPa/m)	-	-	0.2	10	50	50	50	-
Shear Stiffness (GPa/m)	-	-	0.02	10	50	50	50	-

A uniform distributed load 10% greater than the respective analytically derived pile shaft resistance (see Table 1) is applied on the top of the pile in 55 loading stages with constant increment (Stage 1 is a zero load stage). The zero-tip resistance was achieved by allowing the nodes at the lower end (tip) of the pile to freely move downwards in the void. The fixed horizontal but free vertical components of displacement at the tip of the pile, in essence, create an opening in the lower external boundary. The diameter of the opening is a few millimeters greater than the diameter of the pile itself, allowing, therefore, a thin soil shear zone to be created around the pile. Shearing the soil mass itself (instead of the pile-soil interface) corresponds to the α_i=1 case and, in practice, to a bored, cast in-situ, concrete pile (Figure 4, Example 1 in Table 2). The pile is weightless; thus, each staged load on pile corresponds to the respective mobilized shaft resistance.

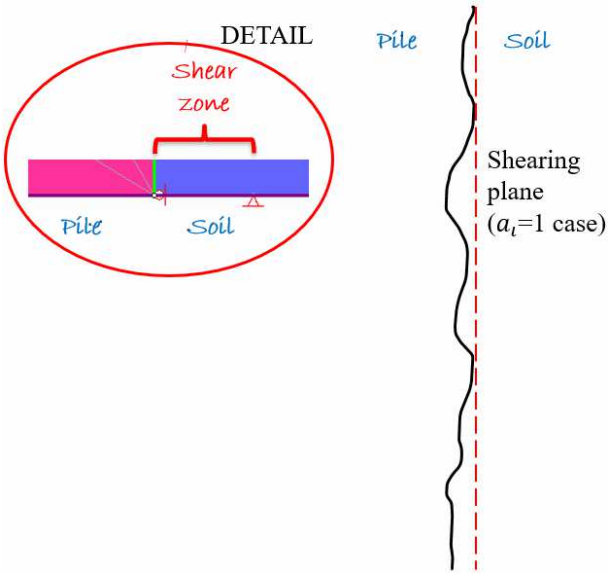

Figure 4. Shearing zone and shearing plane in the pile soil interface.

The numerical 'staged loading on pile' against 'pile settlement' curve has been drawn in Figure 5. A second '$\kappa = \Delta q/\sqrt{\Delta\rho}$' versus 'settlement' curve has also been drawn in the same chart, facilitating in identifying the failure load; the latter corresponds to the shaft resistance capacity of pile. The $\kappa = \Delta q/\sqrt{\Delta\rho}$ parameter is used instead of the rather more apparent local gradient $\Delta q/\Delta\rho$ just for making the visual detection of the failure point more convenient. The shaft resistance as this derived by the proposed method is also indicated on the chart. The comparison revealed a relative difference just 2.2%; please compare the numerically derived 2462.6 kPa value with the respective analytical 2518.5 kPa (proposed method).

The very same example was solved again numerically with the only difference that a "joint" element was used for simulating the pile-soil interface. The properties of this joint element are summarized in Table 2; three different normal and shear stiffness pair of values were examined (Examples 2 to 4), while the joint shear strength characteristics are those of the soil.

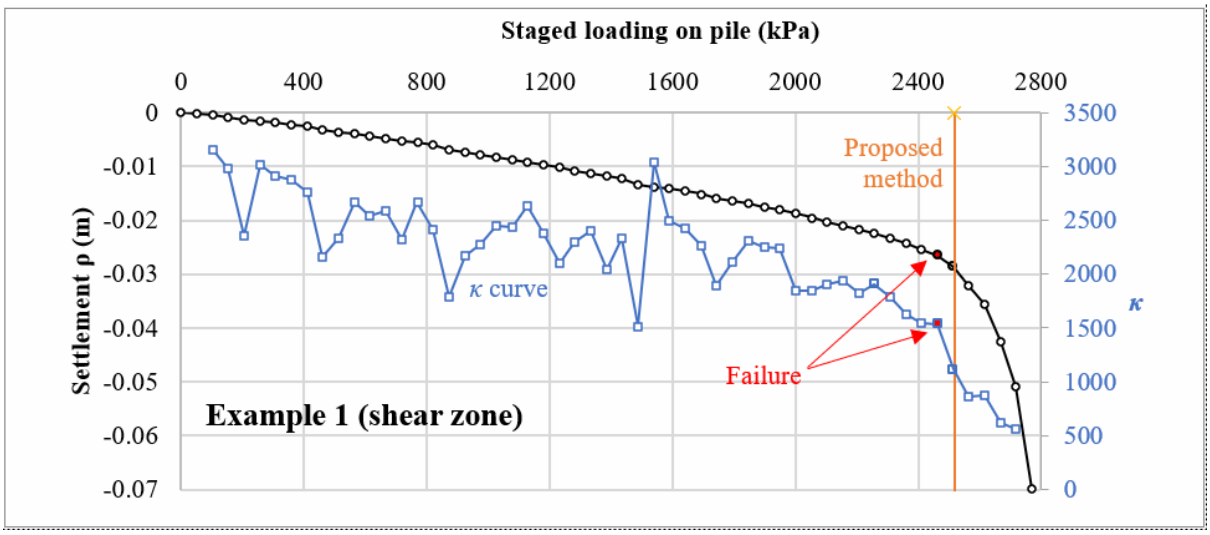

Figure 5. Staged loading on pile against pile settlement or κ; chart referring to Example 1.

Joint stiffness is extremely hard to judge, and getting these parameters is difficult. Because of the lack of reliable data, Rocscience (Rocscience Inc., 2022) suggests as "a good place to start" a normal joint stiffness approximately 10 times the minimum modulus of the two materials on each side of the joint and a shear stiffness approximately the same as the minimum modulus. According again to Rocscience, this generally gives results that are fairly insensitive to the stiffness values, prompting also for a sensitivity analysis for these parameters to be carried out. Using these joint stiffness values (see Example 2 in Table 2), the numerically derived shaft resistance capacity of the pile was 2052.1 kPa, that is, 18.5% lower than the analytical value. The loading-settlement and κ-settlement curves are shown in Figure 6a.

Increasing both normal and shear stiffness of joint to one and five times the stiffness of the pile, the relative difference was decreased to 12.4% and 10.3% respectively (see Examples 3 and 4 in Table 2; the derived shaft resistances were found equal to 2206.1 kPa and 2257.4 kPa respectively). These relative difference values rather indicate that the selected joint stiffness

values of the Example 4 give adequately stable results and that, the joint element itself introduced an error 10.3-2.2=8.1% (recall Example 1). Both loading-settlement and κ-settlement curves for Examples 3 and 4 are shown in Figure 6b and 6c respectively. For comparison reasons, the two loading-settlement curves of Examples 1 and 4 are shown together in the same chart in Figure 7, indicating very good agreement.

Finally, a α_i =2/3 and 1/3 interface strength reduction factor was applied to the RS2 pile model of Example 4 (see Examples 5 and 6 respectively), while all other parameters were kept the same. The loading-settlement and κ-settlement curves for these two new examples are shown in Figure 8a and 8b respectively. The relative difference values found this time were 10.4% and 8.3% respectively (see Examples 5 and 6 in Table 3; the numerically derived shaft resistance capacities were 1504.9 kPa and 768.8 kPa respectively).

All comparison values are summarized in Table 3.

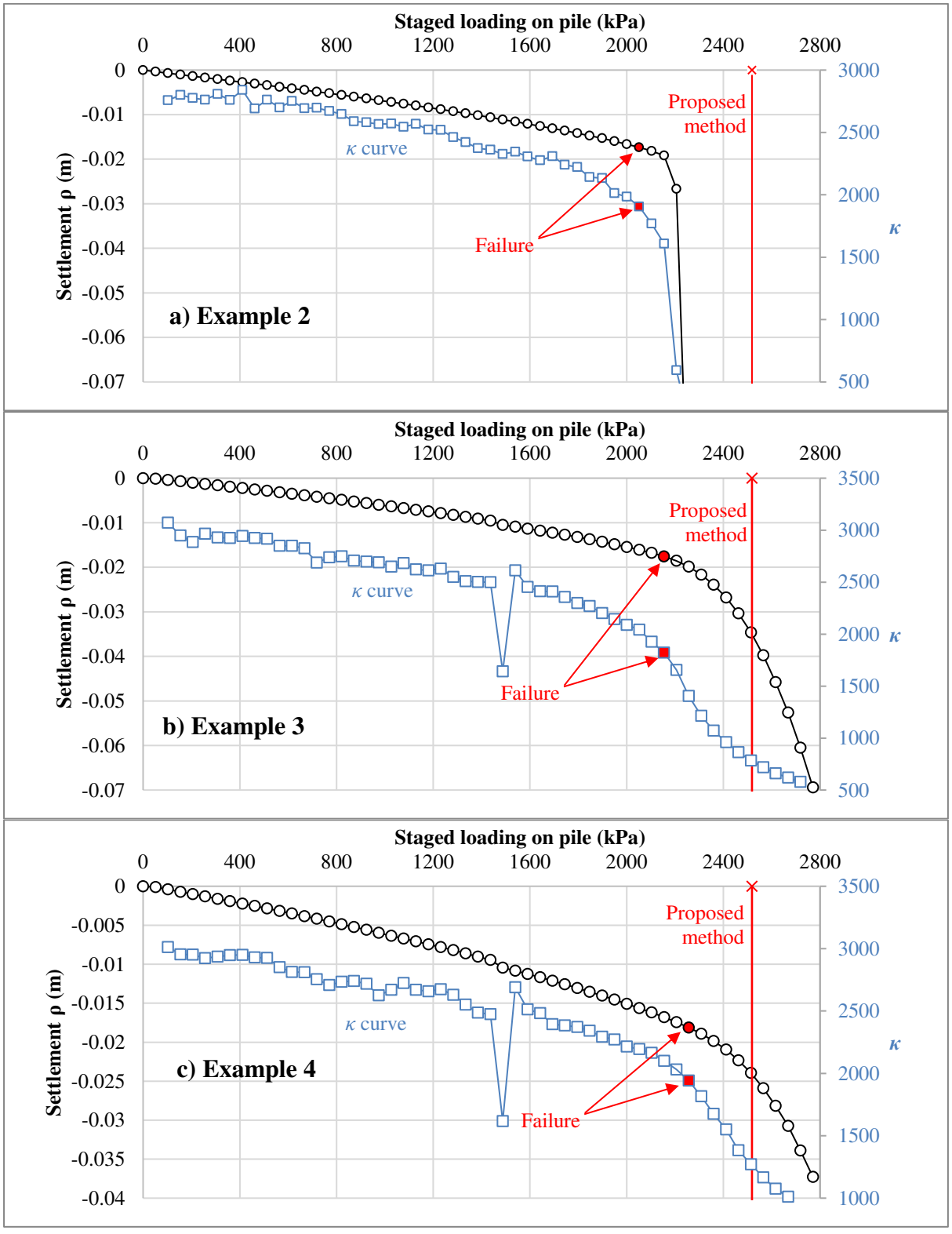

Figure 6. Staged loading on pile against pile settlement or κ; chart referring to Examples 2 to 4 (figure a to c respectively).

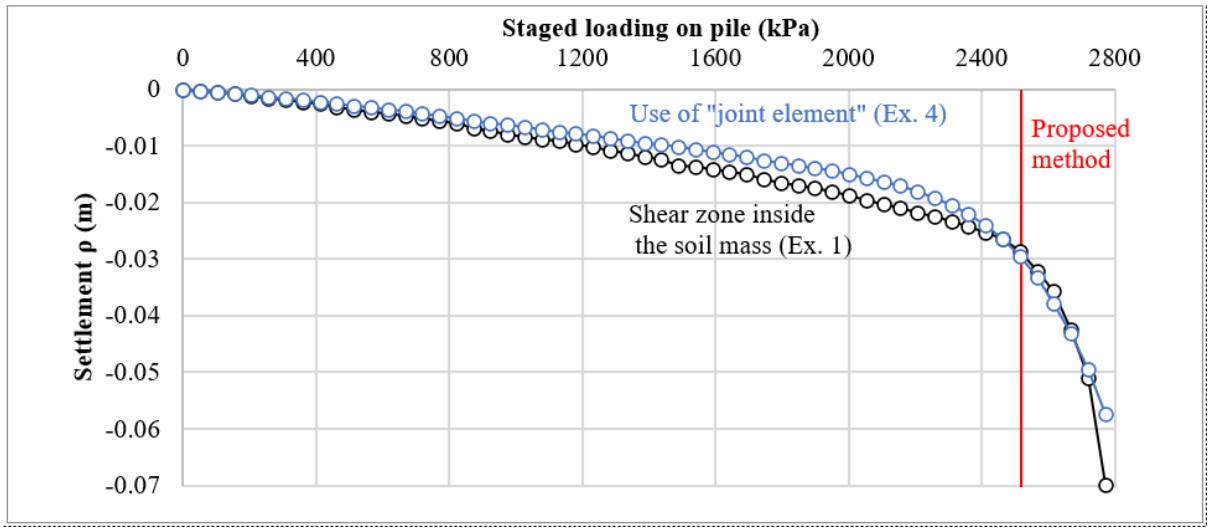

255

256 *Figure 7. Staged loading on pile against pile settlement; chart referring to Examples 1 to 4.*

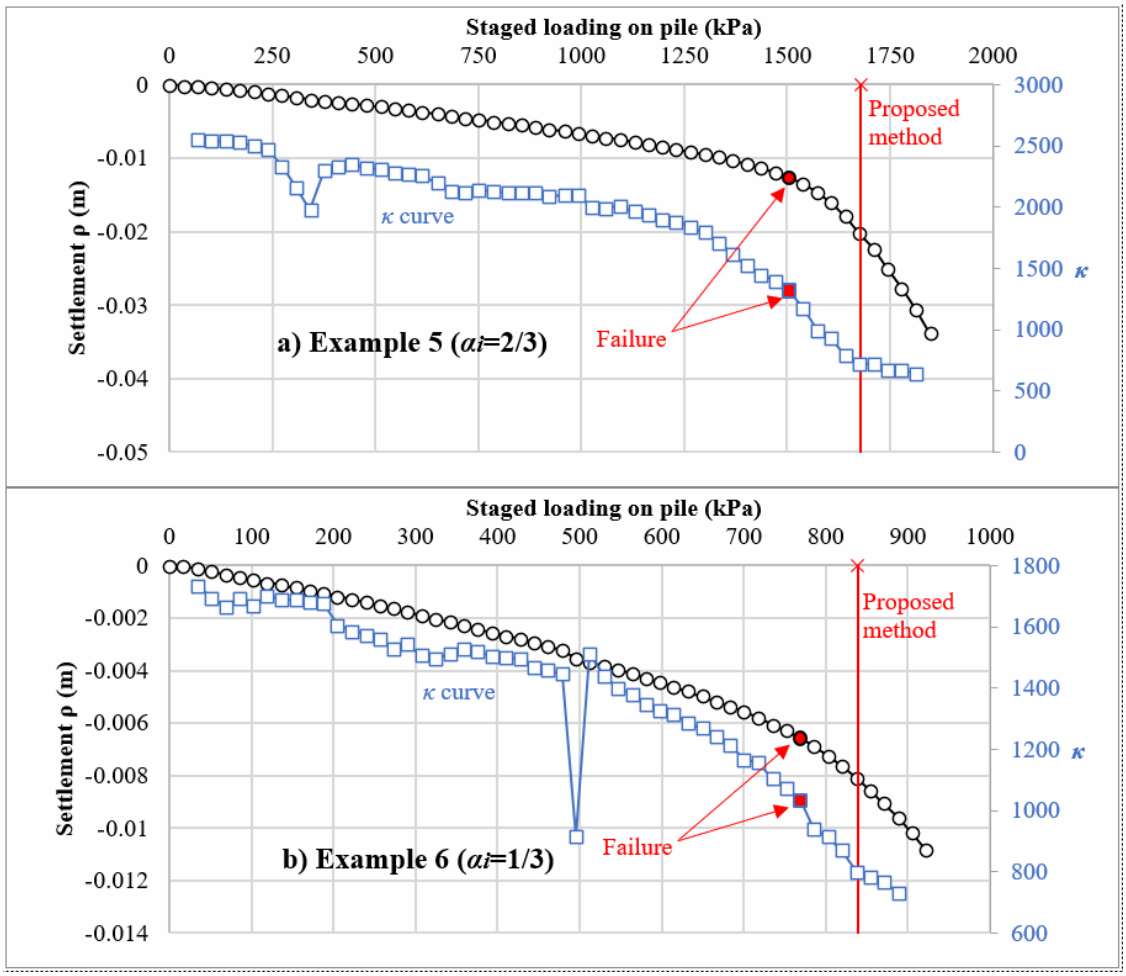

257

258 *Figure 8. Staged loading on pile against pile settlement or κ; chart referring to Examples 5 and 6 (figure a to b respectively).*

259

Table 3. Examples 1 to 6: Shaft resistance capacities of pile. Comparison table.

	Ex. 1	Ex. 2	Ex. 3	Ex. 4	Ex. 5	Ex. 6
Shear reduction coef, α_i	1	1	1	1	2/3	1/3
Normal stiffness of joint (GPa/m)	-	0.2	10	50	50	50
Shear stiffness of joint (GPa/m)	-	0.02	10	50	50	50
Proposed (analytical) (kPa)	2518.5	2518.5	2518.5	2518.5	1679.0	838.7
RS2 (numerical) (kPa)	2462.6	2052.1	2206.1	2257.4	1504.9	768.8
Relative difference	2.2%	18.5%	12.4%	10.3%	10.4%	8.3%

3.2 Tip resistance of pile in a c'=40 kPa, φ'=10° soil

Once the shaft resistance has been calculated independently of the tip resistance of pile, the determination of the tip resistance is now feasible through the total resistance of pile (shaft-tip combined resistance obtained numerically). The lower boundary in Example 1 was, therefore, moved to a new position (significantly lower), allowing the undisturbed development of the failure mechanism in the vicinity of pile tip. The geometry and boundary conditions, as well as the mesh and the basic settings used are shown in Figure 9. The loading-settlement and κ-settlement curves are shown in Figure 10. According to the latter, the pile tip resistance for the specific example is 814.8 kPa (shaft resistance= 2518.5 kPa; total resistance= 3333.3 kPa).

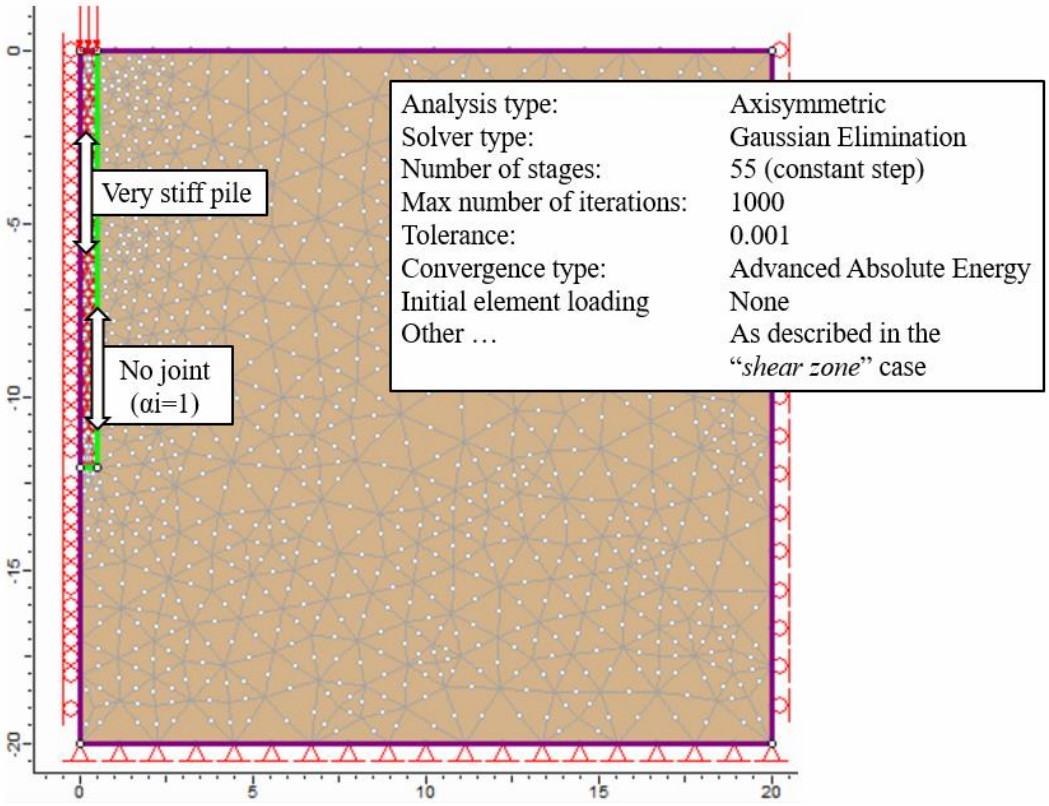

Figure 9. Geometry, boundary conditions, mesh and basic settings for the example referring to the pile with both shaft and tip resistance.

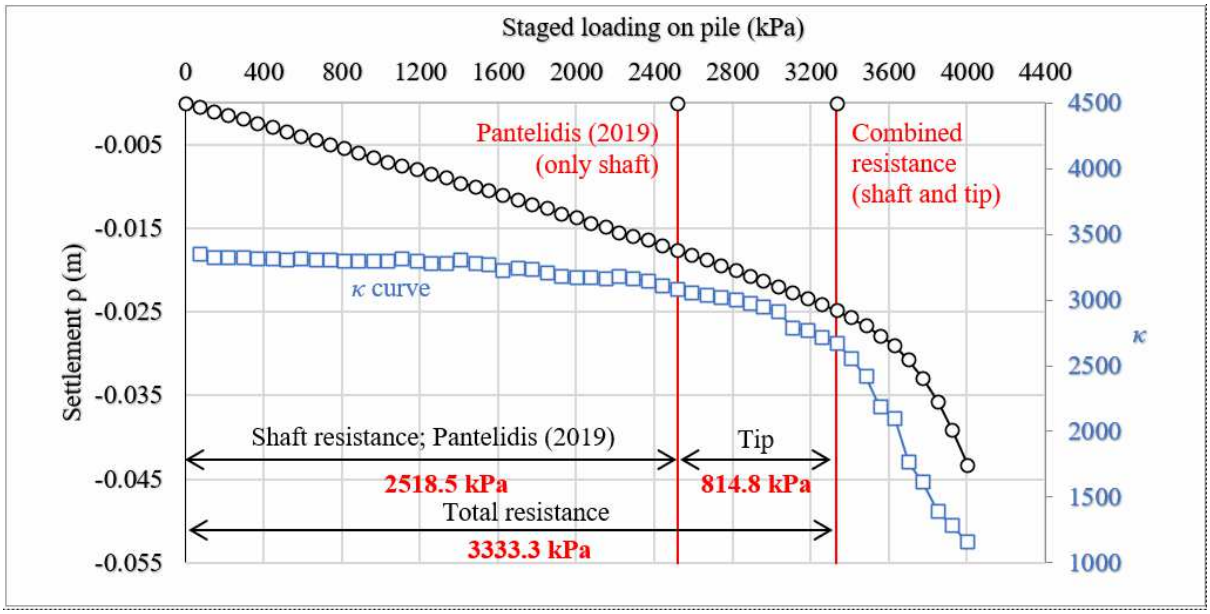

Figure 10. Staged loading on pile against pile settlement or κ; calculation of the tip resistance of pile in a c'=40 kPa, φ'=10° soil.

3.3 Tip and shaft resistance of pile in a c'=40 kPa, φ'=40° soil

In the previous examples the cohesion of soil was set to 40 kPa for emphasizing that in cohesive-frictional soils the $K_{OE} - z$ relationship may significantly deviate from linearity and that, a neutral zone of zero lateral earth pressure exists immediately below the surface. However, one may say that an internal friction angle of soil as low as 10° could be approximated by a total stress analysis, ignoring the friction component. In this respect, for the case of Example 1, Equation 8 would give a shaft resistance capacity 1508.0 kPa, which is significantly lower than the previously obtained 2518.5 kPa value (40.1% relative difference).

Assuming, on the other hand, a much higher phi value, let say, 40°, the analytically derived pile shaft resistance is 2923.6 (see Table 4), while the respective numerically derived value is 2888.8 kPa (see Figure 11). The relative difference between these two values is just 1.2%. In addition to the loading-settlement and κ-settlement curves for the shaft resistance of the pile, Figure 11 shows the respective curves for the total resistance of the latter. According to these curves, the tip resistance for the example examined herein is 5222.2-2923.6=2298.6 kPa.

Deriving dimensionless values for determining the tip resistance of pile is a problem currently under investigation by the author.

Table 4. Table for the calculation of the total resistance of pile shaft based on the proposed method. Asymptotic values (i.e., for z→∞): SMF=0.641, K_{OE}=0.357.

z_{up} (m)	SMF	$K_{OE,up}$*	z_{down} (m)	SMF	$K_{OE,down}$	$\overline{K_{OE}}$	Δz (m)	$\bar{z}$ (m)	$Q_{s,i}$ (kN)
col.1	col.2	col.3	col.4	col.5	col.6	col.7	col.8	col.9	col.10
0	0	(-0.204)	1.678	0.321	0	0	1.678	0.839	210.9
1.678	0.321	0	3	0.431	0.089	0.0445	1.322	2.339	173.4
3	0.431	0.089	4	0.478	0.134	0.1115	1	3.5	146.2
4	0.478	0.134	6	0.530	0.192	0.163	2	5	337.3
6	0.530	0.192	8	0.558	0.227	0.2095	2	7	406.0
8	0.558	0.227	12	0.586	0.266	0.2465	4	10	1022.5
				Total shaft resistance force, Q_s (kN)					2296.2
				Total resistance of pile shaft, $q_{s,tot}$ (kPa)					2923.6

* Negative K_{OE} values in the calculations of the pile shaft resistance are replaced with zero.

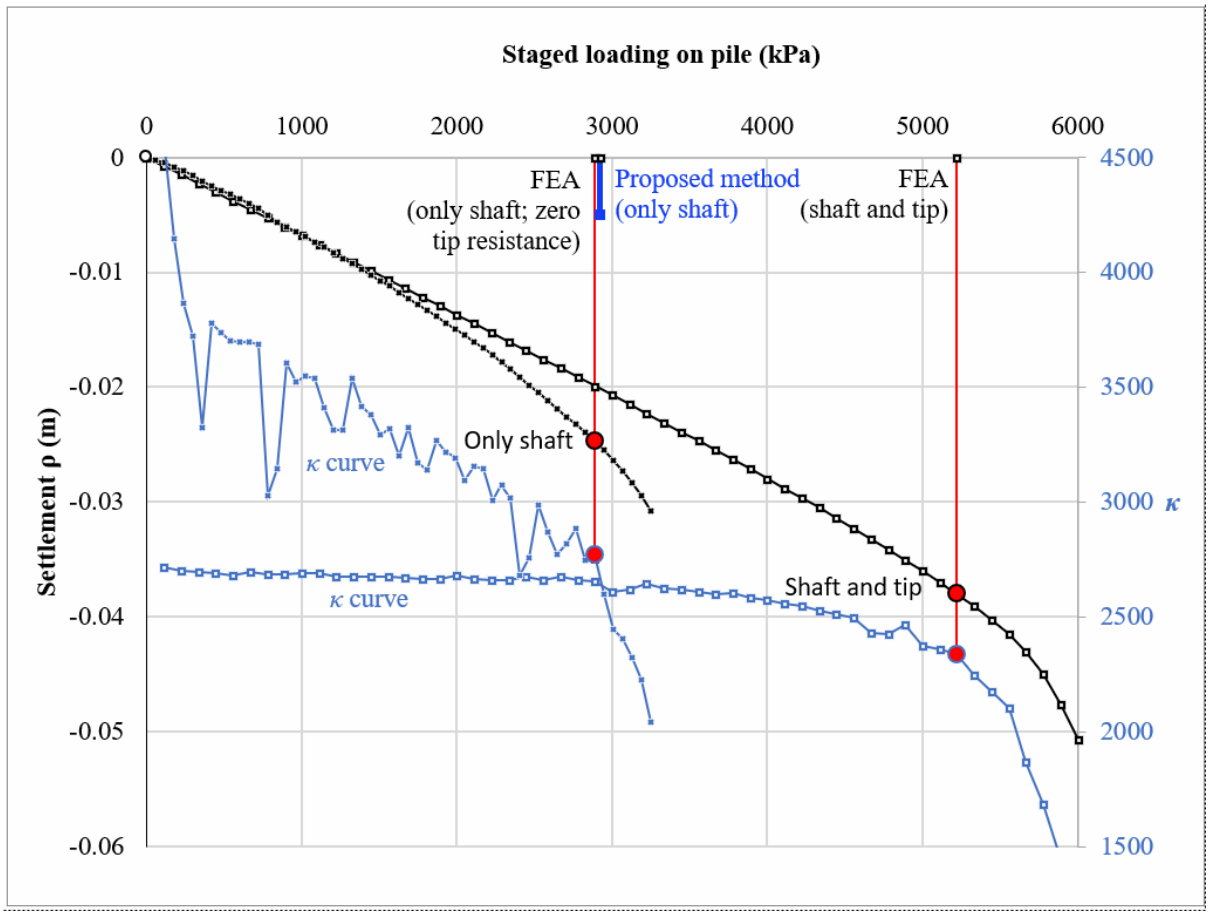

Figure 11. Staged loading on pile against pile settlement or κ; calculation of the tip resistance of pile in a c'=40 kPa, φ'=40° soil.

5. Conclusions

According to the current practice, the shaft resistance of piles based on ground parameters is calculated with the α- method or the β-method, for total or effective stress conditions respectively. And while the physics behind the α-method and the β-method is adequate for calculating the shaft resistance of piles in clays and sands for total and effective stress analysis respectively, the main difficulty in applying the effective stress approach in clays is to estimate the radial effective stress acting on the pile. In the present paper, this is addressed by the suggested coefficient of earth pressure at-rest derived from a continuum mechanics approach. This coefficient is applicable to cohesive-frictional soils and both horizontal and vertical pseudo-static conditions.

Comparison examples show that the analytically derived shaft resistance capacities deviate by only a few percentage points from the respective numerical ones; such relative difference values can, apparently, be attributed to the common modelling error. Indeed, when the pile-soil interface is modelled as a thin shear zone inside the soil mass (no "joint" element, just shearing the soil), the relative difference is negligible. When a "joint" element is used for numerically modelling the pile-soil interface, a sensitivity analysis is necessary for the proper selection of the normal and shear moduli of the joint element, so that the error to be kept in acceptable levels.

Regarding seismic conditions it is noted that, for the case of axially loaded piles the horizontal component of a seismic excitation does not affect the shaft resistance capacity of piles at all, while the vertical component could be neglected as acting favorably. In this respect, a

321 k_v pseudo-static coefficient acting downwards, increases the weight of the pile and of the su-
322 perstructure (unfavorable actions), while increasing the interface shearing resistance (favorable
323 action).

324 Finally, it is mentioned that the proposed method could be used as a general $c - \varphi$ procedure,
325 applicable also to the cases covered by the α-method and the β-method.

326 **Appendix**

327 SMF and K_{OE} values are given in Table 5 and 6 respectively. These values are for the $\{k_h = 0,$
328 $k_v\}$ situation and for various λ_K- φ' combinations, where λ_K is defined as follows:

329 $$\lambda_K = (1 - k_v)\gamma z/c' \quad (18)$$

330 *Table 5. SMF values for different λ_K- φ' combinations ($k_h = 0$).*

λ_K	φ' (°)									
	0	5	10	15	20	25	30	35	40	45
0.005	0.002	0.003	0.003	0.003	0.003	0.003	0.003	0.003	0.003	0.003
0.02	0.010	0.010	0.011	0.011	0.011	0.012	0.012	0.012	0.012	0.012
0.05	0.024	0.025	0.026	0.027	0.028	0.028	0.029	0.029	0.029	0.029
0.1	0.048	0.049	0.051	0.053	0.054	0.055	0.056	0.056	0.057	0.057
0.2	0.090	0.094	0.097	0.100	0.103	0.105	0.106	0.107	0.107	0.106
0.3	0.128	0.133	0.138	0.142	0.146	0.149	0.151	0.151	0.152	0.150
0.4	0.161	0.168	0.175	0.180	0.184	0.188	0.190	0.191	0.191	0.190
0.5	0.191	0.199	0.207	0.213	0.218	0.223	0.225	0.227	0.227	0.225
0.7	0.240	0.250	0.260	0.268	0.275	0.281	0.285	0.287	0.287	0.285
1	0.293	0.306	0.318	0.329	0.338	0.345	0.351	0.354	0.355	0.354
1.5	0.349	0.364	0.379	0.392	0.404	0.414	0.422	0.428	0.431	0.431
2	0.382	0.399	0.415	0.430	0.444	0.455	0.465	0.473	0.478	0.480
3	0.419	0.438	0.455	0.472	0.487	0.501	0.513	0.522	0.530	0.535
4	0.438	0.458	0.476	0.494	0.510	0.524	0.537	0.549	0.558	0.565
5	0.450	0.470	0.489	0.507	0.524	0.539	0.552	0.564	0.575	0.583
10	0.475	0.496	0.515	0.534	0.552	0.568	0.583	0.596	0.608	0.619
20	0.488	0.509	0.529	0.548	0.565	0.582	0.598	0.612	0.625	0.636
50	0.495	0.516	0.536	0.556	0.574	0.591	0.607	0.621	0.634	0.646
100	0.498	0.519	0.539	0.558	0.576	0.594	0.609	0.624	0.638	0.650
200	0.499	0.520	0.540	0.560	0.578	0.595	0.611	0.626	0.639	0.652
500	0.500	0.521	0.541	0.560	0.579	0.596	0.612	0.627	0.640	0.653

331

332

Table 6. K_{OE} *values for different* λ_K*-* φ' *combinations* ($k_h = 0$).

λ_K	φ' (°)									
	0	5	10	15	20	25	30	35	40	45
0.005	0.002	-0.039	-0.077	-0.110	-0.139	-0.162	-0.181	-0.195	-0.203	-0.205
0.02	0.010	-0.032	-0.070	-0.104	-0.133	-0.157	-0.175	-0.189	-0.197	-0.200
0.05	0.025	-0.018	-0.056	-0.091	-0.120	-0.145	-0.164	-0.178	-0.187	-0.191
0.1	0.050	0.006	-0.034	-0.069	-0.100	-0.126	-0.146	-0.161	-0.171	-0.175
0.2	0.099	0.053	0.010	-0.028	-0.061	-0.089	-0.112	-0.129	-0.141	-0.148
0.3	0.147	0.098	0.053	0.013	-0.023	-0.054	-0.079	-0.099	-0.114	-0.123
0.4	0.193	0.141	0.094	0.051	0.013	-0.021	-0.049	-0.072	-0.089	-0.100
0.5	0.236	0.183	0.133	0.087	0.046	0.010	-0.021	-0.046	-0.066	-0.080
0.7	0.315	0.258	0.204	0.154	0.108	0.067	0.031	0.000	-0.025	-0.044
1	0.414	0.352	0.293	0.237	0.185	0.137	0.095	0.058	0.026	0.000
1.5	0.535	0.468	0.402	0.340	0.281	0.226	0.175	0.130	0.089	0.055
2	0.618	0.547	0.478	0.411	0.347	0.287	0.231	0.180	0.134	0.094
3	0.721	0.645	0.572	0.500	0.431	0.365	0.303	0.245	0.192	0.145
4	0.781	0.703	0.626	0.552	0.480	0.410	0.345	0.284	0.227	0.176
5	0.820	0.740	0.662	0.586	0.511	0.440	0.372	0.309	0.250	0.196
10	0.905	0.822	0.740	0.659	0.581	0.505	0.433	0.364	0.300	0.242
20	0.951	0.866	0.782	0.699	0.618	0.540	0.465	0.395	0.328	0.267
50	0.980	0.894	0.808	0.724	0.642	0.562	0.486	0.413	0.345	0.282
100	0.990	0.903	0.817	0.733	0.650	0.570	0.493	0.420	0.351	0.288
200	0.995	0.908	0.822	0.737	0.654	0.574	0.496	0.423	0.354	0.290
500	0.998	0.911	0.825	0.739	0.656	0.576	0.499	0.425	0.356	0.292

Notation

α = adhesion factor for piles in soil

α_i= shear reduction coefficient

$\beta = K_s \tan\delta$ is an empirical coefficient

γ= the unit weight of soil

Δq= incremental loading on pile

$\Delta\rho$= pile displacement due to Δq

δ= the friction angle between the pile and the soil

θ= angle between the earth pressure at-rest, acting radial on the pile and the direction of the horizontal excitation

$\kappa = \Delta q/\sqrt{\Delta\rho}$

346 $\lambda_K = (1 - k_v)\gamma z/c'$

347 $\xi = (\mathrm{m} - 1)/(\mathrm{m} + 1) - 1$

348 σ_{OE} = the at rest earth pressure in the seismic situation

349 φ'= the effective internal friction angle of soil

350 φ_m= the mobilized friction angle of soil (for its calculation see Pantelidis, 2019)

351 φ_{int}= the friction angle at the pile-soil interface

352 c'= the effective cohesion of soil

353 c_m= the mobilized cohesion of soil (for its calculation see Pantelidis, 2019)

354 c_{int}= the cohesion (adhesion) at the pile-soil interface

355 H= the pile length

356 Ko = Jaky's (static) coefficient of earth pressure at rest

357 K_{OE} = the at-rest coefficients of earth pressure in the seismic situation

358 K_{OE}^{+} or K_{OE}^{-}= the earth pressure coefficient at-rest K_{OE} for a positive and negative horizontal

359 pseudo-static coefficient (e.g., for k_h and -k_h)

360 K_s = an earth pressure coefficient

361 K_{XE} = the basic earth pressure coefficient expression (Pantelidis, 2019)

362 k_h= the seismic coefficient of horizontal acceleration

363 k_v= the seismic coefficient of vertical acceleration

364 m=real positive number ranging from 1 to $+\infty$

365 $P_{OE} = P_{OE}^{+} + P_{OE}^{-}$

366 P_{OE}^{+} or P_{OE}^{-} = the at-rest resultant earth pressure force on the pile in the seismic situation refer-

367 ring to the active and the passive "side" respectively

$Q_{s,i}$= the shaft resistance capacity force of the ith sublayer

Q_s= the total shaft resistance capacity force

q_s= unit resistance of pile shaft

$q_{s,tot}$= total resistance of pile shaft

SMF=Strength Mobilization Factor

R= the radius of pile

T = different period of vibration

z= the depth where the earth pressure is calculated

z_{nz}= the depth of neutral zone

Data availability statement

All data used are available from the corresponding author by request.

Declaration of Competing Interest

The author declare that they have no known competing financial interests or personal relationships that could have appeared to influence the work reported in this paper.

References

AASHTO (American Association of State Highway and Transportation Officials), 2010. LRFD Bridge Design Specifications, 5th ed. Washington, DC.

API, 2000. Recommended Practice 2A-WSD. Planning, Designing, and Constructing Fixed Offshore - Working Stress Design (21st edition; including errata and supplement un to 3, August 2007). Washinigton.

Bell, A.L., 1915. The lateral pressure and resistance of clay and the supporting power of clay foundations. In: Minutes of the Proceedings of the Institution of Civil Engineers. Thomas Telford-ICE Virtual Library, pp. 233–272.

391 Burland, J., 1973. Shaft friction of piles in clay--a simple fundamental approach. Publ. Gr. Eng.
392 6.
393 Jaky, J., 1944. The coefficient of earth pressure at rest. J. Soc. Hungarian Archit. Eng. 355–
394 388.
395 Jaky, J., 1948. Pressure in silos. In: Proceedings of the 2nd International Conference on Soil
396 Mechanics and Foundation Engineering ICSMFE. London, pp. 103–107.
397 Mayne, P.W., Kulhawy, F.H., 1982. K0-OCR relationships in soil. J. Geotech. Eng. 108 (GT6),
398 851–872.
399 Mononobe, N., Matsuo, H., 1929. On the determination of earth pressures during earthquakes.
400 In: World Engineering Congress. Tokyo.
401 Okabe, S., 1926. General theory of earth pressure. Japan Soc. Civ. Eng. 12.
402 Pantelidis, L., 2019. The Generalized Coefficients of Earth Pressure: A Unified Approach.
403 Appl. Sci. 9, 5291.
404 Pantelidis, L., Christodoulou, P., 2022. Comparing Eurocode 8-5 and AASHTO methods for
405 earth pressure analysis against centrifuge tests, finite elements, and the Generalized
406 Coefficients of Earth Pressure. ResearchSquare (preprint).
407 https://doi.org/10.21203/rs.3.rs-1808466/v2
408 prEN1997-3:2021, 2021. Eurocode 7 - Geotechnical design - Part 3: Geotechnical structures
409 (draft standard).
410 Rankine, W.J.M., 1857. II. On the stability of loose earth. Philos. Trans. R. Soc. London 9–27.
411 Rocscience Inc., 2022. RS2: Joints [WWW Document]. URL
412 https://www.rocscience.com/help/rs2/documentation/knowledge-base/joints (accessed
413 6.9.22).

414 Tien, N.T., 1981. Design of piles in cohesive soil. Statens Geotekniska Institut (SGI),
415 Linköping.
416 Tomlinson, M.J., 1957. The adhesion of piles driven in clay soils. In: Proceedings of the 4th
417 International Conference on Soil Mechanics and Foundation Engineering. pp. 66–71.
418